Bridge System Performance Assessment from Structural Health Monitoring: A Case Study

Ming Liu, M.ASCE[1]; Dan M. Frangopol, F.ASCE[2]; and Sunyong Kim[3]

Abstract: Based on the long-term monitored strain data induced by heavy vehicle traffic on an existing bridge, this paper presents an efficient approach to assessing the bridge system performance through a series-parallel system model consisting of bridge component reliabilities. The correlations among the bridge component safety margins are obtained by using actual traffic and strain data from structural health monitoring (SHM). The prediction of bridge system reliability in the future is dependent on the performance functions of components. Sensitivity studies with respect to system modeling, correlations, extreme value probability distributions, measurement errors, and number of observations are carried out. A case study of the proposed approach is provided on an existing highway bridge in Wisconsin, which was monitored in 2004 by the Advanced Technology for Large Structural Systems Center, a National Engineering Research Center at Lehigh University, Bethlehem, Pa, USA. This study provides a solid basis for integrating SHM data into practical assessment of bridge system performance.

DOI: 10.1061/(ASCE)ST.1943-541X.0000014

CE Database subject headings: Bridges; Structural reliability; Structural safety; Monitoring; Assessments.

Introduction

Structural health monitoring (SHM) of a bridge can provide abundant information on bridge component conditions and system performance. Current SHM procedures are facing many challenges. For example, one has to decide what has to be monitored and how to do it when preparing for SHM. Accessibility is the most difficult matter during installing SHM, and the monitored data can be timely processed only under clearly defined procedures. Nevertheless, the greatest challenge in an efficient SHM design is how to integrate the monitored data into bridge management systems in order to achieve the goals of SHM. In general, the objectives of SHM include: (1) to detect potential structural damage; (2) to predict the remaining service life of a structure as accurately as possible; (3) to provide the database for optimal maintenance decision process in order to avoid costly replacement; and (4) to help the transition of structural design methodology from current semiprobabilistic load resistance factored design to future probabilistic performance-based design. Depending on the goals of SHM, the procedures to analyze identical sets of the monitored data may be different. Therefore, it is crucial to develop an objective-oriented methodology to effectively process the monitored data. Since bridge system reliability is an important performance measure in bridge safety evaluation (Frangopol and Estes 1997), this paper presents a system reliability-based approach to processing SHM data for the purpose of satisfying the goals above. An illustration is provided by using an actual bridge (see Fig. 1) over the Wisconsin River (I-39 Bridge, Northbound) that was monitored between July and November 2004 by the Advanced Technology for Large Structural Systems (ATLSS) Center, a National Engineering Research Center at Lehigh University, Bethlehem, Pa, USA. The approach proposed is applied to the monitored data obtained from the four strain gauges (CH 3, CH 4, CH 5, and CH 6) indicated in Fig. 1.

This paper focuses on the development of the procedure for assessing bridge system reliability through a series-parallel system model that consists of bridge component reliabilities. The bridge component reliabilities are obtained from the long-term monitored strain data induced by heavy vehicle traffic on a bridge. The correlations among the bridge component safety margins are studied by using actual traffic and strain data from SHM. The prediction of bridge system performance is dependent on the performance functions of components. Sensitivity studies with respect to system modeling, correlations, extreme value probability distributions, measurement errors, and number of observations, are carried out. This study provides a solid basis for integrating SHM data into practical assessment of bridge system performance. It is emphasized that the success in estimating system performance from SHM data depends on how accurately the structural system is modeled in terms of all critical components.

Bridge Performance Assessment Based on Monitored Strain Data

The bridge performance assessment in this study includes the assessments of the bridge component reliabilities as well as the bridge system reliability. The bridge component reliability can be

[1]Research Associate, Dept. of Civil and Environmental Engineering, ATLSS Center, Lehigh Univ., 117 ATLSS Dr., Bethlehem, PA 18015-4729. E-mail: mil307@lehigh.edu

[2]Professor and Fazlur R. Khan Endowed Chair of Structural Engineering and Architecture, Dept. of Civil and Environmental Engineering, ATLSS Center, Lehigh Univ., 117 ATLSS Dr. Bethlehem, PA 18015-4729 (corresponding author). E-mail: dan.frangopol@lehigh.edu

[3]Graduate Research Assistant, Dept. of Civil and Environmental Engineering, ATLSS Center, Lehigh Univ., 117 ATLSS Dr., Bethlehem, PA 18015-4729. E-mail: suk206@lehigh.edu

Note. This manuscript was submitted on March 24, 2008; approved on December 19, 2008; published online on May 15, 2009. Discussion period open until November 1, 2009; separate discussions must be submitted for individual papers. This paper is part of the ***Journal of Structural Engineering***, Vol. 135, No. 6, June 1, 2009. ©ASCE, ISSN 0733-9445/2009/6-733–742/$25.00.

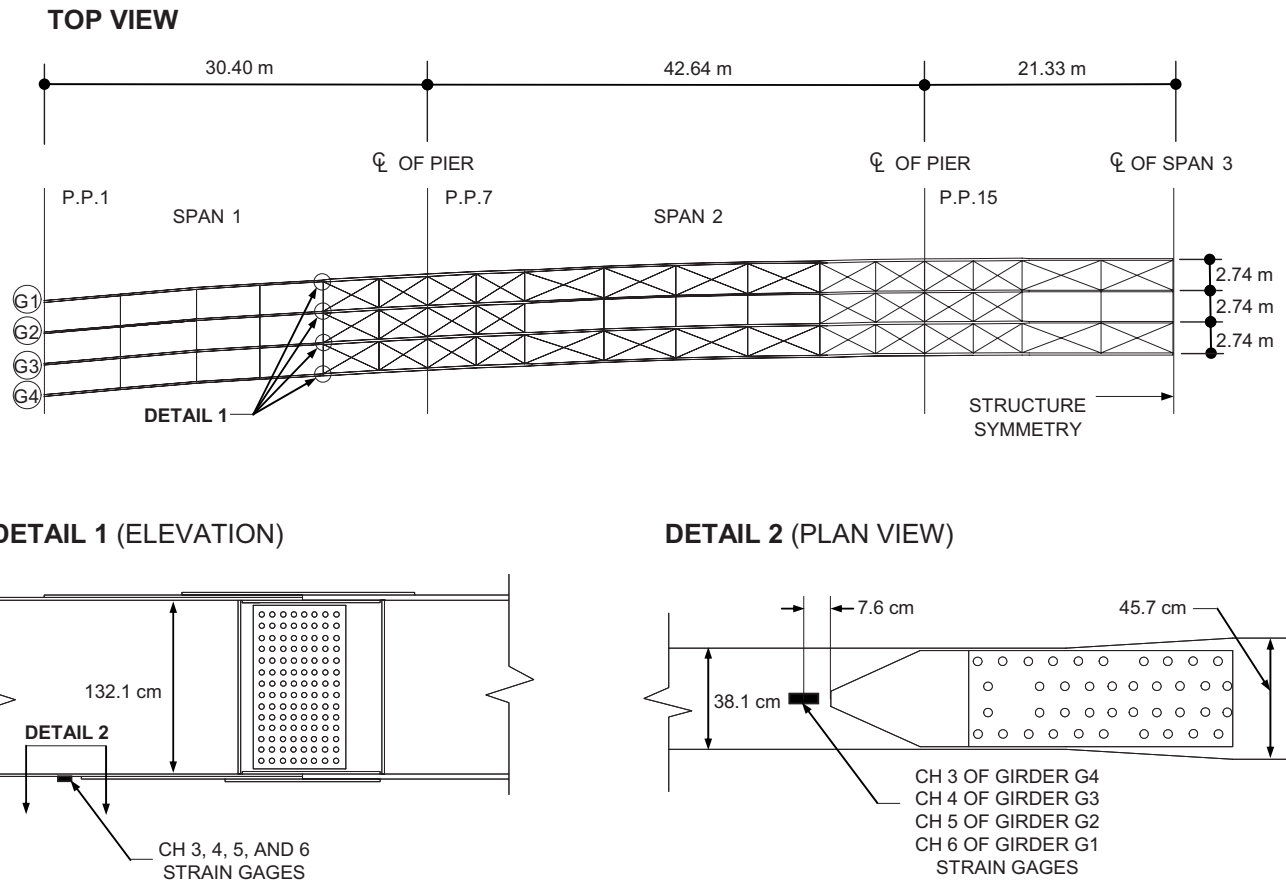

Fig. 1. Sensor locations on the I-39 Northbound Wisconsin River Bridge (adapted from Mahmoud et al. 2005)

obtained from the monitored strain data by using the limit state equation (Liu et al. 2009)

$$g = \varepsilon_o(s,t) - (1+e) \times \zeta(s,t) \times \varepsilon(s,t) = 0 \tag{1}$$

where s=spatial coordinates of the critical location; $\varepsilon_o(s,t)$ =predefined strain limit at time t at the critical location s, which can be assigned as either the yield strain of the component material or the maximum strain from the experimental studies; $\zeta(s,t)$ =time-variant function at the critical location s, which may be used to predict future strain $\varepsilon(s,t)$ through the probability distributions of the extreme values, such as Gumbel, Fisher-Tippett, or Weibull; e=measurement error in the monitored data, which can be assumed to have the normal probability distribution with mean 0.0 and standard derivation σ_e, i.e., $N(0,\sigma_e)$; and $\varepsilon(s,t)$ =component strain at time t, which can be derived from the monitored strain data as

$$\varepsilon(s,t) = \frac{1}{m} \times \sum_{i=1}^{m} (\varepsilon_i(s_i,t) \times \alpha_i(s_i,t)) \tag{2}$$

where m=number of the strain gauges on the same component; $\varepsilon_i(s_i,t)$=strain readings from the ith strain gauge at time t; and $\alpha_i(s_i,t)$=condition function for the ith strain gauge at time t. The condition function $\alpha_i(s_i,t)$ is used to estimate $\varepsilon(s,t)$ when the strain gauge locations are different from the critical locations. This condition function can be estimated by consideration of results of condition assessment, locations of strain gauge, and failure mode. For example, suppose that a simply supported beam is under vertical loads, its failure mode is assumed to be by bending, and two strain gauges 1 and 2 are installed on the bottom of the beam at locations l_1 and l_2. If the results of the condition assessment show that the critical location l_{cr} is different from the locations where these two strain gauges are installed, $\alpha_i(s_i,t)$ in Eq. (2) can be estimated by using the condition function as

$$\alpha_1(s_1,t) = \frac{M_{cr}(t) \cdot d_{cr}}{M_1(t) \cdot d_1} \times \frac{I_1(t)}{I_{cr}(t)} \tag{3a}$$

$$\alpha_2(s_2,t) = \frac{M_{cr}(t) \cdot d_{cr}}{M_2(t) \cdot d_2} \times \frac{I_2(t)}{I_{cr}(t)} \tag{3b}$$

where d_{cr}, d_1, and d_2=the distances from the centroid of the cross sections to the bottom of the beam at locations l_{cr}, l_1, and l_2, respectively, and $M_{cr}(t)$, $M_1(t)$, and $M_2(t)$=the bending moments at time t associated with cross sections at locations l_{cr}, l_1, and l_2, respectively. These bending moments can be obtained by performing a structural analysis or by field test. $I_{cr}(t)$, $I_1(t)$, and $I_2(t)$=moments of inertia at time t associated with locations l_{cr}, l_1, and l_2, respectively. They can be estimated from condition assessment. If all strain gauge locations are at the critical locations, $\alpha_i(s_i,t)$=1.0. However, this assumption may be unconservative from a structural reliability viewpoint; in fact, the critical locations and critical components in a structural system are dependent on the loading conditions and deterioration mechanisms. It is important to recognize that a rational estimation of system performance from SHM data depends on how correctly and completely the structural system is modeled in terms of all critical components. Obviously, this can be accomplished by using structural identification prior to the SHM application.

In this study, the predictions of future bridge performance are based on the statistics of extremes, which states that when the number of SHM data, k, is large enough, the extreme value distribution of the SHM data will asymptotically approach one of the following three probability distributions: (a) Gumbel distribution; (b) Fisher-Tippett distribution; and (c) Weibull distribution, regardless of the original probability distributions of the SHM data (Ang and Tang 1984). The Gumbel probability distribution (Gumbel 1958)

$$F(\varepsilon_\chi) = \exp\left(-\exp\left(-\frac{\varepsilon_\chi - \lambda}{\eta}\right)\right) \quad -\infty < \varepsilon_\chi < +\infty \tag{4}$$

is adopted herein, where $F(\varepsilon_\chi)$=cumulative distribution function of the Gumbel probability distribution; ε_χ=extreme value of a random variable ε [i.e., the maximum value of ε_i ($i=1,2,3,\ldots,k$)]; λ and η=constants to be determined from the measured data by either theory of order statistics or graphical method. Thus, the extreme values of the SHM data in the future, $\varepsilon_\chi(T)$, can be predicted as (Ang and Tang 1984)

$$\varepsilon_\chi(T) = \lambda - \eta \cdot \ln\left[-\ln\left(1 - \frac{1}{T}\right)\right] \tag{5}$$

where T=return period, and the ratio $\zeta(s,t)$ is defined as

$$\zeta(s,t=T) = \frac{\varepsilon_\chi(T)}{\max(\varepsilon_1, \varepsilon_2, \ldots, \varepsilon_k)} \tag{6}$$

where $\zeta(s,t)$ will be assigned as 1.0 when the computed value of $\zeta(s,t)$ from Eq. (6) is less than 1.0 for conservative considerations. As a result, the future component reliabilities of the bridge can be predicted through Eqs. (1)–(6), considering the expected service lifetime.

Bridge system reliability can be assessed by using bridge component reliabilities obtained from Eq. (1) through a simplified series-parallel system model (Liu and Frangopol 2005). A series system fails when any of its components fail, while a parallel system fails only after all of its components fail. This study extensively uses the RELSYS (RELiability of SYStems), a computer program developed at the University of Colorado (Estes and Frangopol 1998).

Sensitivity Studies

It has been recognized that many factors influence bridge system reliability assessment based on monitored strain data. For example, transverse positions of heavy vehicle traffic greatly affect the probability distributions of the monitored strain data on each girder for multiple girder bridges. The computed component and system reliabilities may be sensitive to the fitting probability functions adopted. The number of observations (e.g., the monitored strain data) determines the lengths of the monitoring periods. Obviously, the minimal operational costs of a SHM system can be obtained when the shortest required monitoring periods are established in advance. Moreover, the measurement errors may have considerable effects on the outputs of the proposed procedures. In this study, all reliability assessment is conducted by using the loading patterns from both single and side-by-side heavy vehicle traffic, and the sensitivity studies are carried out for different system models by varying the number of the bridge components involved. The fitting probability functions adopted include the generalized extreme value (GEV), lognormal, and beta probability distributions indicated in Eqs. (7)–(9), respectively

$$f_X(x) = \frac{1}{\sigma}\left[1 + \xi\left(\frac{x-\eta}{\sigma}\right)\right]^{-1/\xi-1} \times \exp\left(-\left[1 + \xi\left(\frac{x-\eta}{\sigma}\right)\right]^{-1/\xi}\right) \quad \begin{matrix}\sigma > 0 \\ 0 < \sigma + \xi(x-\eta)\end{matrix} \tag{7}$$

$$f_Y(y) = \frac{1}{\sqrt{2\pi}\delta(y-\chi)} \exp\left(-\frac{1}{2}\left(\frac{\ln(y-\chi)-\mu}{\delta}\right)^2\right) \quad \chi < y < +\infty \tag{8}$$

$$f_Z(z) = \frac{1}{B(p,q)} \frac{(z-a)^{p-1}(b-z)^{q-1}}{(b-a)^{p+q-1}} \quad \begin{matrix}a \leqslant z < b \\ p,q > 0\end{matrix} \tag{9}$$

where $f_X(x)$=probability density function (PDF) of the GEV distribution; ξ=shape parameter of $f_X(x)$; σ=scale parameter of $f_X(x)$; η=location parameter of $f_X(x)$. $f_Y(y)$=PDF of the lognormal distribution; μ=mean of $\ln(y-\chi)$; δ=standard deviation of $\ln(y-\chi)$; χ=location parameter of $f_Y(y)$; $f_Z(z)$=PDF of the beta distribution; p and q=shape parameters of $f_Z(z)$; a and b=lower and upper bounds of z; and $B(p,q)$=beta function defined as

$$B(p,q) = \int_0^1 x^{p-1}(1-x)^{q-1}dx = \frac{\Gamma(p)\Gamma(q)}{\Gamma(p+q)} \quad p,q > 0 \tag{10}$$

where $\Gamma(\cdot)$=gamma function. All of the parameters mentioned above, (i.e., ξ, σ, η, μ, δ, χ, p, q, a, and b), can be determined from the achievable monitored data by either theory of order statistics or graphical method. Finally, the effects of the number of observations and measurement errors on the outputs of the proposed approach are extensively investigated by using the monitored strain data, actual heavy vehicle traffic information, and rational assumptions.

Case Study

Description of I-39 Northbound Wisconsin River Bridge

The proposed approach is applied to an actual bridge over the Wisconsin River (Bridge I-39, Northbound) in Wisconsin. According to Mahmoud et al. (2005), the I-39 Northbound Wisconsin River Bridge is a five-span continuous steel girder bridge, which has the slightly curved span lengths of 30.40 m (109.6 ft), 42.64 m (139.9 ft), 42.66 m (140.0 ft), 42.64 m (139.9 ft), and 30.40 m (109.6 ft). The horizontal curved bridge has two northbound traffic lanes with four steel plate girders spacing at 2.74 m (9.0 ft) equally (see Fig. 1). The builtup steel girders are a combination of the top and bottom flange plates and a typical 132.1 cm (52 in.) high web plate. The steel flange plates vary from 38.1 cm (15 in.) to 45.7 cm (18 in.) in width, and 3.175 cm (1.25 in.) to 4.445 cm (1.75 in.) in thickness. The steel used in the girders is M270 Grade 50W with the nominal yield strength of 345 MPa (50 ksi). The bridge was opened to traffic in 1961, and carried the average daily traffic from 2,165 to 14,500 during the period from 1964 to 2001 (Wisconsin DOT, 2002).

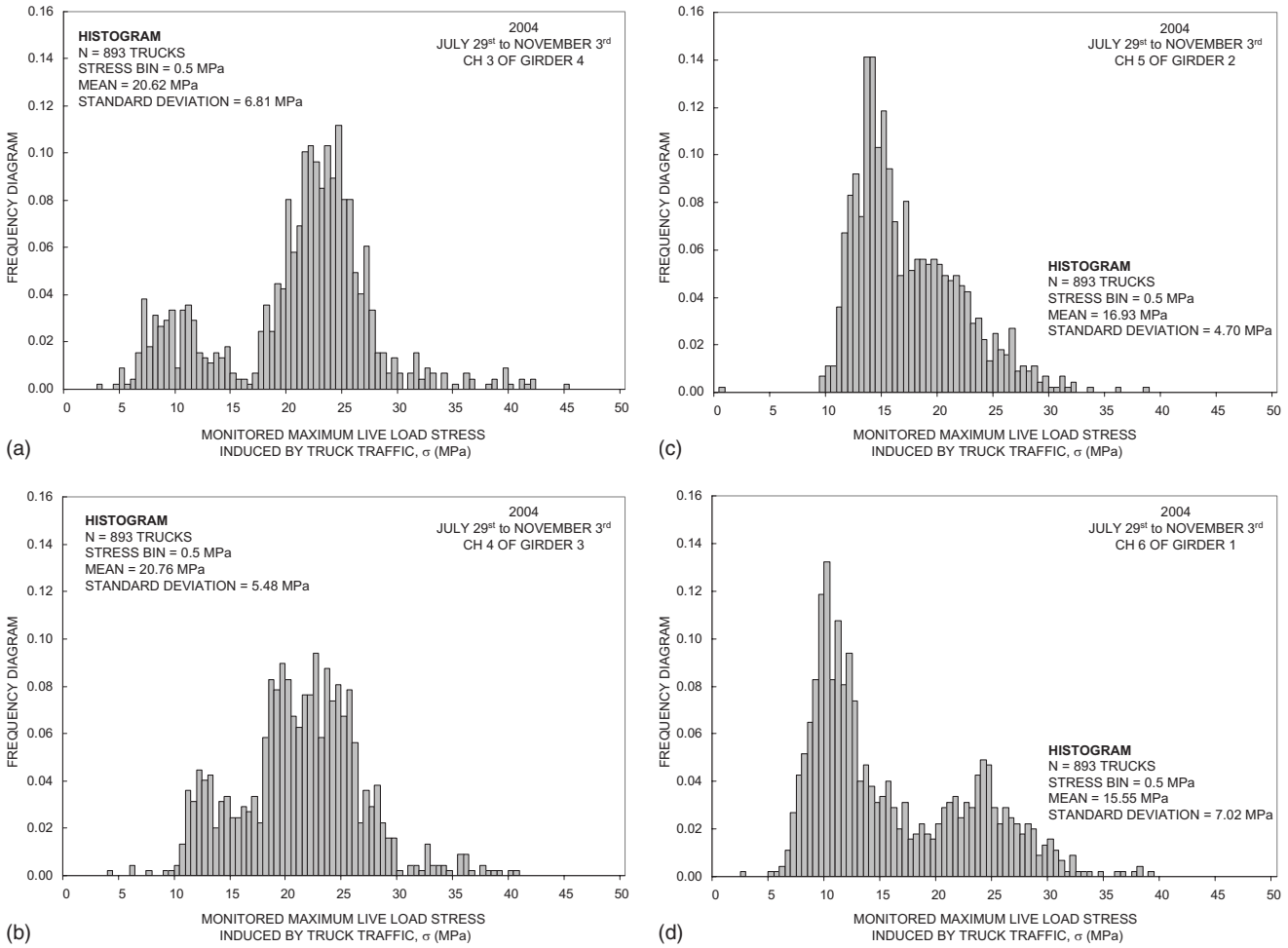

Fig. 2. Histograms of monitored data from (a) CH 3 of Girder 4; (b) CH 4 of Girder 3; (c) CH 5 of Girder 2; and (d) CH 6 of Girder 1

Monitoring Program

The SHM program on this bridge was conducted between July and November 2004 by the personnel from the ATLSS Center with three main objectives (Mahmoud et al. 2005): (a) to assess the bridge serviceability through a complete fatigue evaluation for various fatigue prone details; (b) to estimate the remaining fatigue life of the details in question; and (c) to monitor the structural responses of the bridge under the actual traffic (uncontrolled load tests) for a relatively long period up to 3 or 4 months. There were 24 resistance strain gauges fully temperature compensated by applying the recommended thermal expansion coefficients for structural steel and two linear variable differential transformers installed at 24 locations on the bridge. The controlled load tests including crawl tests [speed up to 8 km/h (5 mph)] and dynamic tests [speed up to 108 km/h (65 mph)] were performed between 9 a.m. and 11 a.m. on July 28, 2004, by employing two triaxle dump trucks with the gross vehicle weights of 296.5 kN (67.2 kips) and 329.2 kN (74.6 kips), respectively. The monitored strain data from the uncontrolled load tests were extensively collected and investigated during the period of 95 days from July 29 to November 3, 2004. It should be noted that all the monitored strain data used in this study are converted into the stress data under the assumption that these strain data follow Hooke's law. The details about the monitoring are reported in Mahmoud et al. (2005).

Assessment of Bridge Component Reliability

This study focuses on the monitored data from Channels 3 to 6, which measured and recorded the structural responses of the east exterior Girder (G4), east interior Girder (G3), west interior Girder (G2), and west exterior Girder (G1), respectively. The corresponding sensors were installed at the bottoms of the bottom flanges, and were located about 25.0 m (82.0 ft) north of the central line of the south abutment of the bridge (see Fig. 1). In order to minimize the volume of monitoring data and to consider only the heavy vehicles, recording of the data in Channels 3 to 6 was triggered when the vehicle induced the strain larger than the predefined strain (Mahmoud et al., 2005). There were a total of 893 events captured during the monitoring period of 95 days (i.e., $N_{tt}=893$), of which 636 heavy vehicles crossed the bridge on the right (east) lane (i.e., $N_{rt}=636$), and 249 heavy vehicles crossed the bridge on the left (west) lane (i.e., $N_{lt}=249$). In addition, there were only eight occurrences when the heavy vehicles crossed the bridge side by side (i.e., $N_{ss}=8$) during the entire monitoring period of 95 days. Figs. 2(a–d) present the histograms of the recorded 893 maximum stresses, which clearly demonstrate that the individual girders of a multiple girder bridge may have quite different responses to the identical loading patterns from actual heavy vehicle traffic. For example, since about 70% (i.e., $N_{rt}/N_{tt}=636/893\approx0.71$) heavy vehicle traffic occurred on the right lane, and only less than 30% (i.e., $N_{lt}/N_{tt}=249/893\approx0.28$)

heavy vehicle traffic occurred on the left lane, the highest peaks in Fig. 2(a and d) are located at different stress ranges, indicating that the east exterior Girder (G4) might have experienced greater cumulative damage than the west exterior Girder (G1). Figs. 2(a and d) show two modes, and Figs. 2(b and c) have only one mode. This indicates that the exterior Girders (G1 and G4) may be more sensitive to the transverse positions of the heavy vehicle traffic than the interior Girders (G2 and G3). Therefore, the bridge component reliability assessment should be performed with the considerations of (1) the spatial positions and importance of the bridge components to the entire structural system of the bridge; (2) actual heavy vehicle traffic information; and (3) results of structural condition assessment on the bridge components. In this case study, the probability that the monitored data from the strain gauge do not exceed the predefined limit from controlled test serves as a reliability measure.

Fig. 3 presents the histograms of the maximum stresses σ_m recorded on the east exterior Girder (G4) under the right lane [see Fig. 3(a)], left lane [see Fig. 3(b)], and side by side [see Fig. 3(c)] heavy vehicle loading conditions. The dashed lines in Fig. 3 represent the best fitting probability density function for the histograms, i.e., the GEV distribution, while the solid lines show the measured maximum strains transformed into stresses σ_o from the controlled load tests. Table 1 summarizes the best fitting values of the GEV parameters, and the corresponding exceedance probability $P_{(i)}(\sigma_m > \sigma_o)$, where $i=1$, 2, and 3 represents the loading conditions under the right lane, left lane, and side-by-side heavy vehicle traffic, respectively. According to the theorem of total probability, the total exceedance probability $P(\sigma_m > \sigma_o)$, which is defined as the probability that σ_m is larger than σ_o, can be expressed as

$$P(\sigma_m > \sigma_o) = \frac{N_{rt}}{N_{tt}} P_{(1)} + \frac{N_{lt}}{N_{tt}} P_{(2)} + \frac{N_{ss}}{N_{tt}} P_{(3)} \tag{11}$$

Similarly, the best fitting values of the GEV parameters and corresponding $P(\sigma_m > \sigma_o)$ for Girders G1, G2, and G3 are also summarized in Table 1, where Girder G4 has the highest probability $P(\sigma_m > \sigma_o) = 0.1432$.

Assessment of Bridge System Reliability

The bridge system reliability is assessed by using the series-parallel system model shown in Fig. 4 (System Model II). The coefficients of correlation $\rho(X, Y)$ among the component strains at time t, $\varepsilon(s, t)$, are directly obtained from the monitored data x and y as follows:

$$\rho(X, Y) = \frac{\Sigma(x - \bar{x})(y - \bar{y})}{\sqrt{\Sigma(x - \bar{x})^2 \Sigma(y - \bar{y})^2}} \tag{12}$$

where $\bar{x}$ and $\bar{y}$ are the average values of the monitored data x and y at time t, respectively. Table 2 presents the resulting $\rho(X, Y)$ for all heavy vehicle loading conditions in 2004, based on the actual monitored data. Although $\rho(X, Y)$ may vary with time, depending on the actual monitored data x and y at time t, $\rho(X, Y)$ is considered as time invariant in this study, due to lack of the actual monitored data other than those obtained in 2004. The bridge system reliabilities are also assessed by using System Models I and III shown in Figs. 5 and 6, respectively. It should be noted that the predefined stress limit σ_o in Eq. (1) is treated as the normal distributed random variable with the mean value equal to the maximum stress measured during the controlled load tests, and the coefficient of variation is assigned to be 4% (including dispersion of the measurement errors during the controlled load tests). As stated previously, the measurement errors herein are also considered as normally distributed random variables with the mean value equal to 0.0 and the standard deviation of 4%.

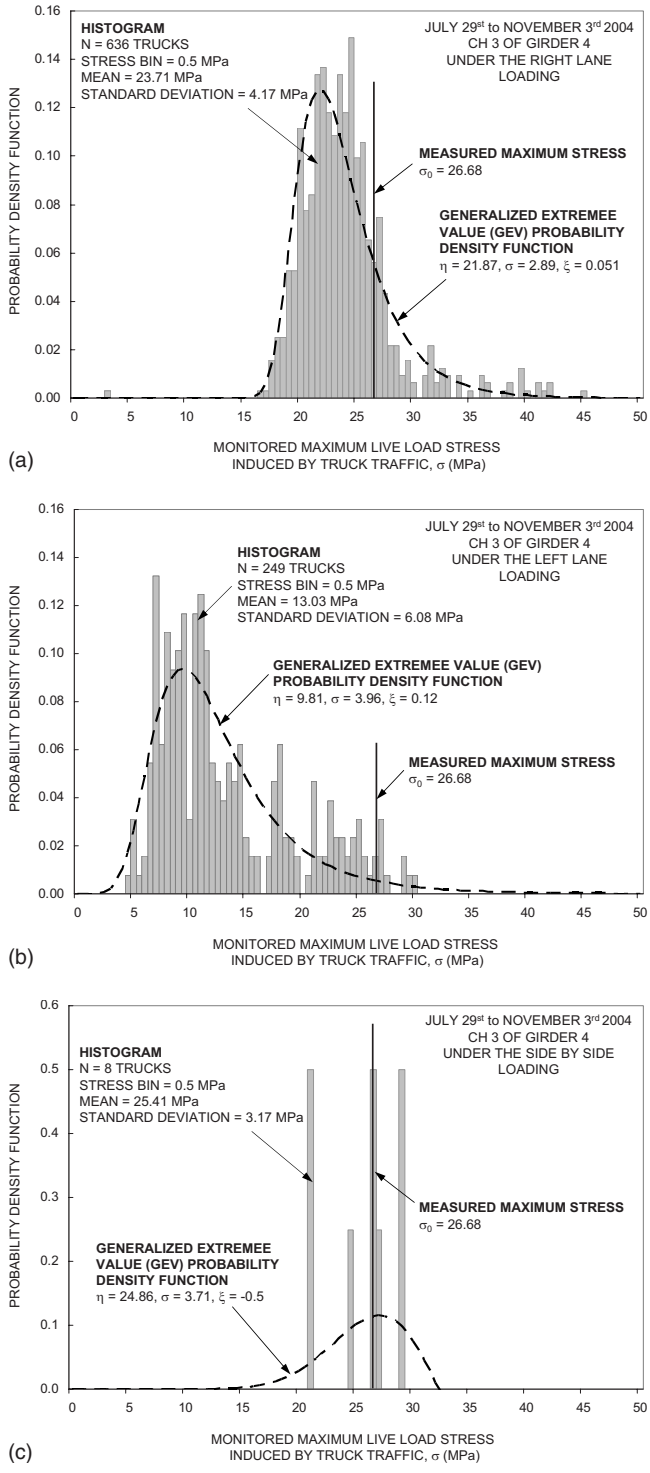

Fig. 3. Histograms and the GEV PDF of monitored data from CH 3 of Girder 4: (a) under the right lane loading; (b) under the left lane loading; and (c) under the side-by-side loading

Table 1. Best Fitting Values for Parameters of the GEV Probability Distributions, and Exceedance Probabilities $P_{(i)}(\sigma_m > \sigma_o)$ and $P(\sigma_m > \sigma_o)$

Girder	G1			G2			G3			G4		
Traffic	Right lane	Left lane	Side by side	Right lane	Left lane	Side by side	Right lane	Left lane	Side by side	Right lane	Left lane	Side by side
η	10.02	23.14	23.57	13.39	20.04	22.01	20.97	13.02	25.37	21.87	9.81	24.86
σ	2.64	3.63	4.90	2.36	3.08	6.21	3.25	3.16	3.12	2.89	3.96	3.71
ξ	0.105	−0.195	0.102	0.104	−0.096	−0.047	−0.036	0.174	0.125	0.051	0.122	−0.658
$P_{(i)}(\sigma_m > \sigma_o)$	0.007	0.226	0.370	0.0070	0.0367	0.2810	0.085	0.028	0.320	0.183	0.032	0.425
$P(\sigma_m > \sigma_o)$		0.07086			0.01772			0.07096			0.14319	

Sensitivity Studies

The resulting exceedance probabilities are 0.002%, 0.012%, and 0.483% for System Models I, II, and III, respectively. Therefore, it may be concluded that the proposed approach is sensitive to the system models adopted.

The effects of the fitting PDFs on the proposed approach are studied by using the GEV, lognormal, and beta distributions. Figs. 7 and 8 compare three distributions for the histograms of the maximum stresses obtained from the west interior Girder (G2) under the right and left lane heavy vehicle loading conditions, respectively. While the GEV distribution provides the best fitting results, the lognormal and beta distributions offer reasonable fitting results, particularly for the left lane loading condition (see Fig. 8). Table 3 compares the computed probabilities $P(\sigma_m > \sigma_o)$ when the GEV, lognormal, and beta distributions are used, respectively. The GEV is associated with the largest computed probabilities for Girders G1, G2, and G3, and with the smallest one for Girder G4. However, the differences in the computed probabilities $P(\sigma_m > \sigma_o)$ as shown in Table 3 are small enough to be ignored. In other words, the proposed approach is almost insensitive to the types of the fitting probability functions, if GEV, lognormal, or beta distribution is adopted.

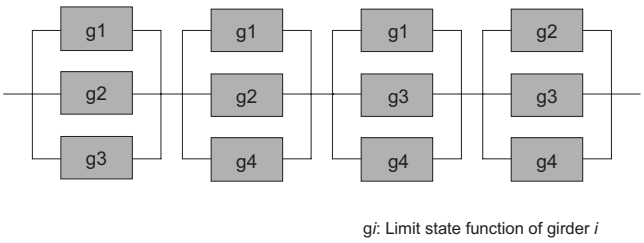

Fig. 4. System Model II of the I-39 Northbound Wisconsin River Bridge

The sensitivity studies with respect to the measurement errors are conducted by varying the values of the standard deviation of the errors from 2% up to 8%. Fig. 9 presents the corresponding exceedance probabilities for System Models I, II, and III. It may be concluded that the increases of the dispersion of the measurement errors may result in increasing the probabilities of exceedance, regardless of the types of the system models adopted. In addition, the probabilities of exceedance with both perfect and zero correlations among the random variables in Eq. (1) are computed for System Models I, II, and III, respectively. Fig. 10 shows that assuming independent random variables in Eq. (1) (i.e., the coefficients of correlation=0.0) yields to smaller probabilities of exceedance of the structural system than those based on the actual coefficients of correlation. Conversely, the assumption of perfect correlations (i.e., the coefficients of correlation=1.0) results in conservative assessment. Thus, it is important to obtain the actual coefficients of correlation directly from the monitored data at time t. Therefore, further research on estimating time-variant coefficients of correlation among the random variables in Eq. (1) is necessary.

Furthermore, the sensitivity studies with respect to the number of observations are extensively conducted by using the entire,

Table 2. Coefficients of Correlation among the Monitored Strain Data

Girder		G1			G2			G3			G4		
	Traffic	Right lane	Left lane	Side by side	Right lane	Left lane	Side by side	Right lane	Left lane	Side by side	Right lane	Left lane	Side by side
G1	Right lane	1.000	0.000	0.000	0.811	0.000	0.000	0.303	0.000	0.000	0.261	0.000	0.000
	Left lane	0.000	1.000	0.000	0.000	0.784	0.000	0.000	0.312	0.000	0.000	0.152	0.000
	Side by side	0.000	0.000	1.000	0.000	0.000	0.973	0.000	0.000	0.307	0.000	0.000	0.511
G2	Right lane	0.811	0.000	0.000	1.000	0.000	0.000	0.531	0.000	0.000	0.422	0.000	0.000
	Left lane	0.000	0.784	0.000	0.000	1.000	0.000	0.000	0.481	0.000	0.000	0.339	0.000
	Side by side	0.000	0.000	0.973	0.000	0.000	1.000	0.000	0.000	0.366	0.000	0.000	0.504
G3	Right lane	0.303	0.000	0.000	0.531	0.000	0.000	1.000	0.000	0.000	0.394	0.000	0.000
	Left lane	0.000	0.312	0.000	0.000	0.481	0.000	0.000	1.000	0.000	0.000	0.915	0.000
	Side by side	0.000	0.000	0.307	0.000	0.000	0.366	0.000	0.000	1.000	0.000	0.000	0.798
G4	Right lane	0.261	0.000	0.000	0.422	0.000	0.000	0.394	0.000	0.000	1.000	0.000	0.000
	Left lane	0.000	0.152	0.000	0.000	0.339	0.000	0.000	0.915	0.000	0.000	1.000	0.000
	Side by side	0.000	0.000	0.511	0.000	0.000	0.504	0.000	0.000	0.798	0.000	0.000	1.000

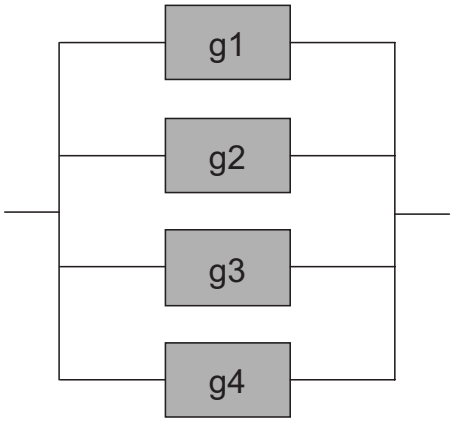

Fig. 5. System Model I of the I-39 Northbound Wisconsin River Bridge

half, and one third of the original monitored data. Since a total of 636 heavy vehicles were captured under the right lane traffic during the monitoring period, the original monitored data associated with these 636 heavy vehicles are divided into three groups consisting of the first, middle, and last 318 heavy vehicles, respectively, where the middle 318 heavy vehicles start at vehicle number 159 (i.e., 636/4) and end at vehicle number 477 (i.e., 159+318). Fig. 11 compares the GEV PDFs for the east interior Girder (G3) under the loading conditions associated with 636 and 318 heavy vehicles on the right lane. These original monitored data are also divided into the five groups consisting of 212 heavy vehicles (i.e., 636/3=212), and Fig. 12 presents the corresponding GEV fitting functions. Table 4 compares the exceedance prob-

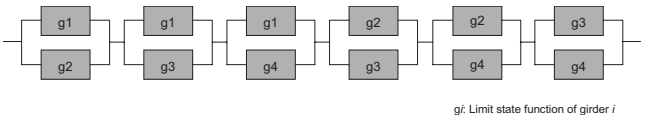

Fig. 6. System Model III of the I-39 Northbound Wisconsin River Bridge

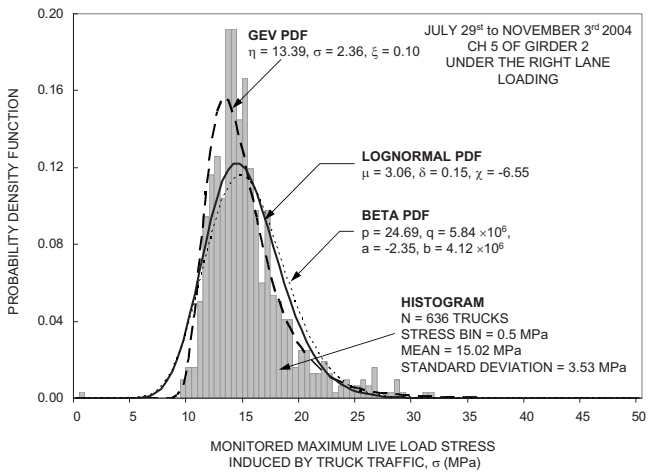

Fig. 7. Comparison of the GEV, lognormal, and beta PDF for CH 5 of Girder 2 under the right lane loading

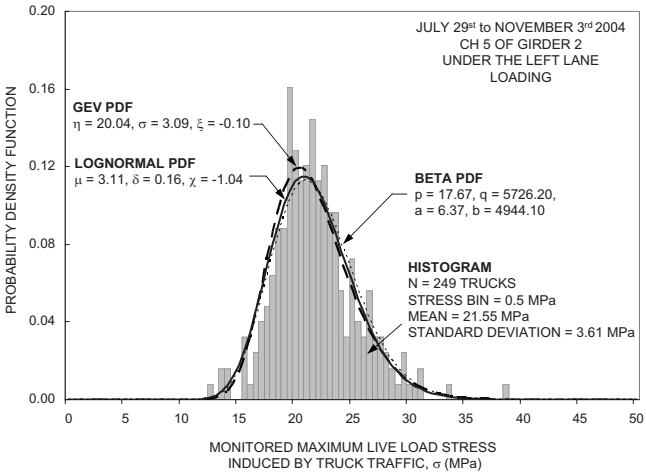

Fig. 8. Comparison of the GEV, lognormal, and beta PDF for CH 5 of Girder 2 under the left lane loading

abilities $P_{(1)}(\sigma_m > \sigma_o)$ for all four Girders (G1, G2, G3, and G4) under the loading conditions associated with 636, 318, and 212 heavy vehicles. Similarly, Table 5 compares the exceedance probabilities $P_{(2)}(\sigma_m > \sigma_o)$ under the loading conditions associated with 249, 125, and 83 heavy vehicles on the left lane traffic. It should be noted that α in Tables 4 and 5 is defined as

$$\alpha = \frac{P_{(i)}(p) - P_{(i)}(o)}{P_{(i)}(o)} \tag{13}$$

where $P_{(i)}(o) = P_{(i)}(\sigma_m > \sigma_o)$ associated with the entire original monitored data, and $P_{(i)}(p) = P_{(i)}(\sigma_m > \sigma_o)$ associated with the partial original monitored data. In general, the more heavy vehicles

Table 3. Comparisons of Exceedance Probabilities $P(\sigma_m > \sigma_o)$ Associated with G1, G2, G3, and G4 for the GEV, Lognormal, and Beta Fitting Functions

Girder	G1	G2	G3	G4
GEV	0.07086	0.01772	0.07096	0.14319
Lognormal	0.06670	0.01176	0.06472	0.16842
Beta	0.06906	0.01336	0.06798	0.17528

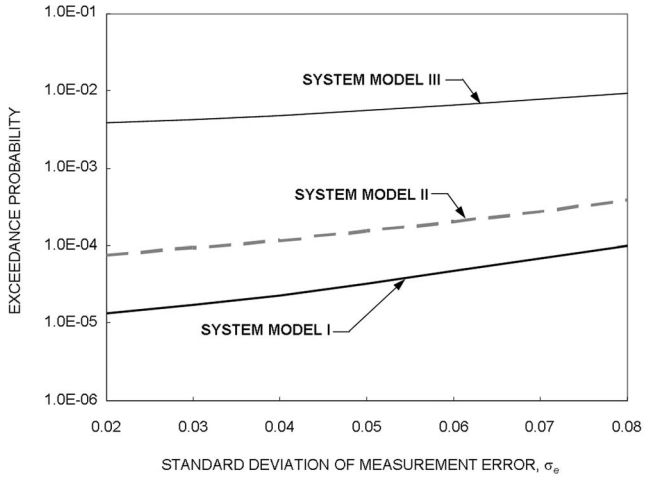

Fig. 9. Effect of measurement error on exceedance probability of System Models I, II, and III

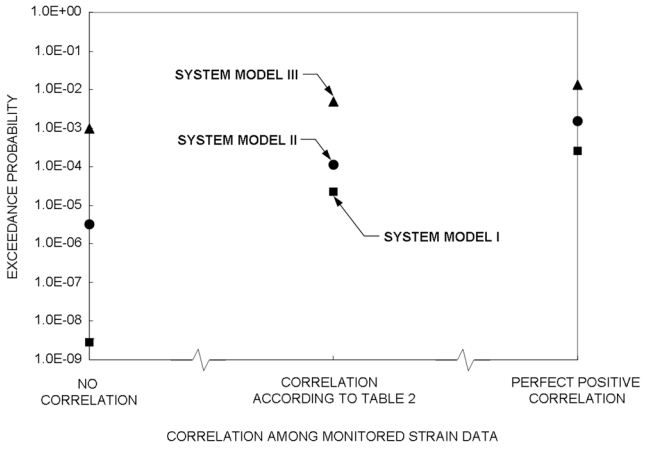

Fig. 10. Effect of correlation among the monitored strain data on exceedance probability of System Models I, II, and III

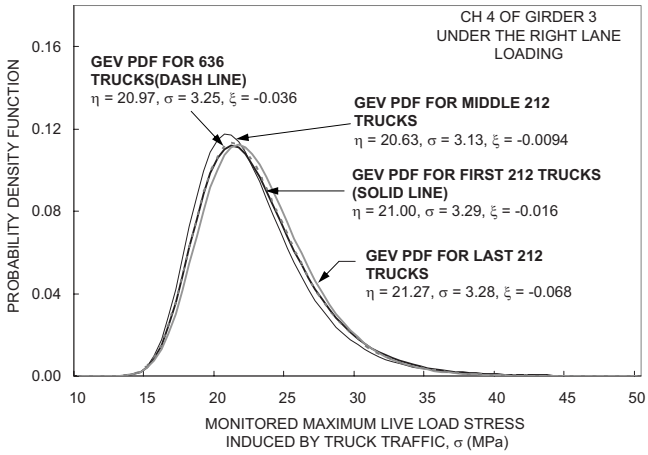

Fig. 12. Effect of number of observations on the GEV PDF for CH 4 of Girder 3 under the right lane loading (636 heavy vehicles versus 212 heavy vehicles)

involved, the more reliable the evaluation of $P_{(i)}(\sigma_m > \sigma_o)$. For example, as shown in Table 5, the difference in $P_{(2)}(\sigma_m > \sigma_o)$ resulting from 249 and 125 heavy vehicles is in the range between −3.7% and 18.8% for G1 under the left lane traffic loading. However, when only 83 (i.e., 249/3=83) heavy vehicles are involved, this difference increases to a wider range from −26.4% to 25.0%. Fig. 13 shows the computed $P_{(1)}(\sigma_m > \sigma_o)$ for G2 under the right lane traffic, which tends to converge to a stable value of 0.0070. When only half of the original monitored data (i.e., 636/2=318) are used in the computations, $P_{(1)}(\sigma_m > \sigma_o)$ ranges between 0.0066 and 0.0075, and the corresponding difference is between −5.7% and 7.1%. In other words, if the predefined acceptable interval estimation of $P_{(1)}(\sigma_m > \sigma_o)$ is within 10% of the exact value, only half the original monitored data (i.e., those associated with 318 heavy vehicles) is required for G2 under the right lane traffic. Similarly, if the predefined acceptable interval estimation increases from 10% to 15%, the number of the original monitored data required may be reduced from 318 to 212, which results in the difference ranging between −10.0% and 12.9% (see Table 4), and the computed $P_{(1)}(\sigma_m > \sigma_o)$ between 0.0063 and 0.0079 as shown in Fig. 13.

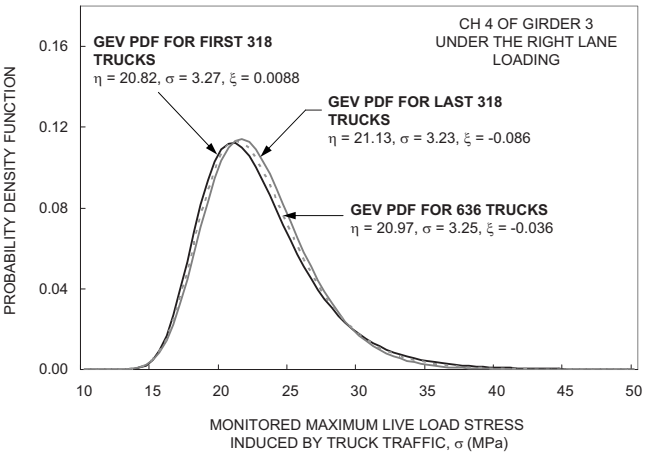

Fig. 11. Effect of number of observations on the GEV PDF for CH 4 of Girder 3 under the right lane loading (636 heavy vehicles versus 318 heavy vehicles)

Prediction of Bridge System Reliability

The exceedance probability associated with the bridge system is predicted by using Eqs. (5) and (6). According to the original monitored data, there were 636 and 249 heavy vehicles captured under the right and left lane traffic, respectively, during the monitoring period of 95 days. Therefore, it is estimated that the annual numbers of heavy vehicles are approximately 2,500 on the right lane and 1,000 on the left lane. Consequently, the total number of passages of the heavy vehicles in the next t years will be $T=2{,}500\times t$ for the right lane, and $T=1{,}000\times t$ for the left lane, where T=return period in Eq. (5). Fig. 14 presents the computed exceedance probabilities associated with the three system models of the bridge at current time (i.e., in 2004) and the predicted probabilities of exceedance during the next 5, 10, 15, and 20 years. It is important to understand that the increase in the exceedance probabilities with time in Fig. 14 are caused by the predicted increases of the load effects from the heavy vehicle traffic only. This is because the original monitored data in this study were collected during the monitoring period of 95 days, and it is reasonable to assume that the deterioration of the bridge conditions during such a short period (95 days) has little effect on the changes of the exceedance probabilities of the bridge system. However, the increase of the time-dependent exceedance probabilities of the system due to the deterioration of the bridge conditions can be also dealt with the proposed approach through the newly developed condition function $\alpha_i(s_i,t)$, as illustrated in Eq. (3).

Conclusions

This paper presented a practical approach to assessing bridge system reliabilities through a series-parallel system model that consists of the bridge components monitored by using SHM. The correlations among the bridge component safety margins were also included by using actual traffic and strain data from SHM. The future system reliabilities of the bridge were predicted by the newly developed component performance function. The sensitivity studies with respect to the system modeling, coefficients of correlations, extreme value probability distributions, measurement errors, and number of observations were extensively carried

Table 4. Comparison of Exceedance Probabilities $P_{(1)}(\sigma_m > \sigma_o)$ for Different Number of Observations under Right Lane Traffic Loading

Girder	G1		G2		G3		G4	
Number of observations	$P_{(1)}$	α^a (%)	$P_{(1)}$	α^a (%)	$P_{(1)}$	α^a (%)	$P_{(1)}$	α^a (%)
636	0.0065	—	0.0070	—	0.0845	—	0.1832	—
First 318	0.0072	10.8	0.0075	7.1	0.0924	9.3	0.1779	−2.9
Last 318	0.0059	−9.2	0.0066	−5.7	0.0751	−11.1	0.1863	1.7
Middle 318	0.0082	26.2	0.0072	3.0	0.0724	−14.3	0.1703	−7.1
First 212	0.0065	0.0	0.0071	1.4	0.0925	9.5	0.1735	−5.3
Middle 212	0.0083	27.7	0.0063	−10.0	0.0749	−11.4	0.1803	−1.6
Last 212	0.0052	−20.0	0.0079	12.9	0.0870	3.0	0.1926	5.1
212 ending at the middle	0.0091	40.5	0.0071	1.4	0.0746	−11.7	0.1628	−11.1
212 starting at the middle	0.0061	−6.2	0.0078	11.7	0.0813	−3.8	0.1887	3.0

[a]See Eq. (13).

out by using the actual SHM data collected in 2004 from an existing highway bridge in Wisconsin. The following conclusions can be drawn from this study.

1. The proposed approach can effectively assess the bridge system performance using the SHM data collected on existing bridges. However, the system models that combine the bridge component performance functions in different series and parallel forms may greatly affect the results. In addition, in order to achieve valuable system performance assessment, it is important to obtain the actual coefficients of correlation among the random variables directly from the monitored data.
2. The GEV probability distribution function provides the best fittings to the histograms that are obtained from the monitored maximum strains under each of the passages of the heavy vehicle traffic. However, the lognormal and beta probability distribution functions can also offer reasonable probabilities associated with the monitored strains exceeding the predefined limits. This is because the computed exeedance probabilities are primarily dependent on the upper tails of the fitting functions, where the GEV, lognormal, and beta distributions are all very similar. Therefore, it may be concluded that the proposed approach is not very sensitive to the fitting probability functions, if GEV, lognormal, and/or beta distributions are used.
3. The increase in the dispersion of measurement errors results in the increase of the computed exceedance probability, regardless of the system models adopted. This is because the measurement errors are related to the degree of uncertainty in assessing system reliability. On the other hand, the increase in the number of observations (i.e., monitored data) involved reduces the uncertainty associated with system reliability assessment. The required minimum number of monitored data may be determined by the predefined acceptable confidence intervals.
4. The system exceedance probability in the future can be predicted by the newly developed bridge component performance function. However, it is important to identify the causes of the predicted changes of the system exceedance probability. If the original monitored data cover a short period of time only, the predicted changes may be dominated by the effects of the loading conditions. Otherwise, the predicted changes may be caused by the combined effects of the loading conditions and deterioration of bridge performance due to environmental stressors such as corrosion. Actual traffic under heavy trucks is affected by many factors. More detailed probabilistic descriptions associated with different time periods of a day, a week, and a year (seasonal) should be considered in future studies.
5. The bridge system reliability assessment should be performed with the considerations of the spatial positions and importance of each bridge component to the entire bridge system. These considerations may be based on actual heavy vehicle traffic information from SHM and results from the structural condition assessment of the bridge components.
6. The success in the bridge system performance assessment

Table 5. Comparison of Exceedance Probabilities $P_{(2)}(\sigma_m > \sigma_o)$ for Different Number of Observations under Left Lane Traffic Loading

Girder	G1		G2		G3		G4	
Number of observations	$P_{(2)}$	α^a (%)	$P_{(2)}$	α^a (%)	$P_{(2)}$	α^a (%)	$P_{(2)}$	α^a (%)
249	0.2255	—	0.0367	—	0.0284	—	0.0319	—
First 125	0.2172	−3.7	0.0355	−3.3	0.0245	−13.7	0.0329	3.2
Last 125	0.2338	3.7	0.0379	3.4	0.0322	13.4	0.0311	−2.6
Middle 125	0.2678	18.8	0.0436	18.7	0.0237	−16.7	0.0270	−15.5
First 83	0.1660	−26.4	0.0277	−24.6	0.0354	24.6	0.0428	34.1
Middle 83	0.2819	25.0	0.0468	27.4	0.0178	−37.4	0.0246	−22.9
Last 83	0.2176	−3.5	0.0351	−4.3	0.0315	10.8	0.0296	−7.2
83 ending at the middle	0.2649	17.5	0.0558	52.1	0.0286	0.6	0.0334	4.8
83 starting at the middle	0.2459	9.0	0.0367	0.0	0.0273	−3.8	0.0274	−14.0

[a]See Eq. (13).

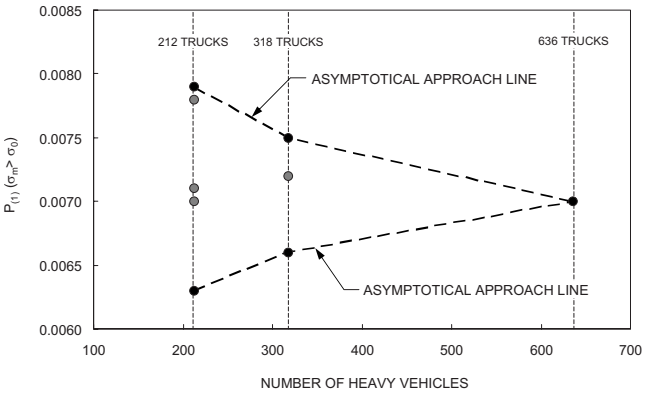

Fig. 13. Comparison of exceedance probabilities $P_{(1)}(\sigma_m > \sigma_o)$ with different number of observations for CH 5 of Girder 2 under the right lane loading

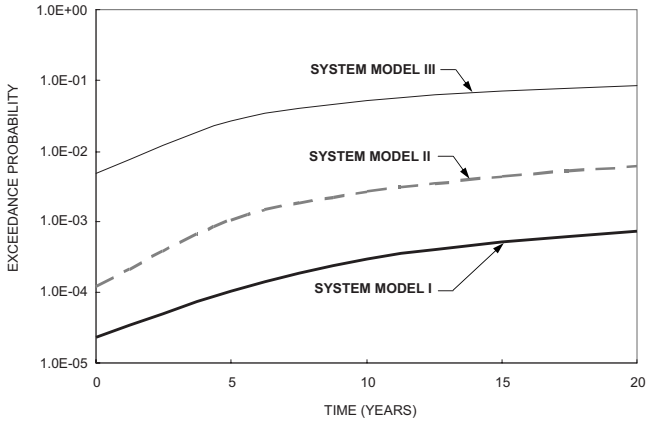

Fig. 14. Time-variant exceedance probabilities of System Models I, II, and III

using SHM data depends on how correctly and completely the bridge system is modeled in terms of all critical components and their contributing response mechanisms. This should be accomplished by a proper structural identification analysis prior to the SHM application.

Acknowledgments

The support from the National Science Foundation through Grant No. CMS-0639428, the Commonwealth of Pennsylvania, Department of Community and Economic Development, through the Pennsylvania Infrastructure Technology Alliance (PITA), and the U.S. Federal Highway Administration Cooperative Agreement Award DTFH61-07-H-00040 is gratefully acknowledged. The writers want to express their profound thanks to Mr. Ian Hodgson, Lehigh University, for his constructive comments and access to the data obtained during the long-term monitoring of the Wisconsin River Bridge I-39. The opinions and conclusions presented in this paper are those of the writers and do not necessarily reflect the views of the sponsoring organizations.

References

Ang, A. H-S., and Tang, H. W. (1984). *Probability concepts in engineering planning and design*, Vol. II, Wiley, New York.

Estes, A. C., and Frangopol, D. M. (1998). "RELSYS: A computer program for structural system reliability analysis." *Struct. Eng. Mech.*, 6(8), 901–919.

Frangopol, D. M., and Estes, A. C. (1997). "Bridge maintenance strategies based on system reliability." *Struct. Eng. Int. (IABSE, Zurich, Switzerland)*, 7(3), 193–198.

Gumbel, E. J. (1958). *Statistics of extremes*, Columbia University Press, New York.

Liu, M., and Frangopol, D. M. (2005). "Time-dependent bridge network reliability: Novel approach." *J. Struct. Eng.*, 131(2), 329–337.

Liu, M., Frangopol, D. M., and Kim, S. (2009). "Bridge safety evaluation based on monitored live load effects." *J. Bridge Eng.*, 14(4), in press.

Mahmoud, H. N., Connor, R. J., and Bowman, C. A. (2005). "Results of the fatigue evaluation and field monitoring of the I-39 Northbound Bridge over the Wisconsin River." *ATLSS Report No. 05-04*, Lehigh Univ., Bethlehem, Pa.

Wisconsin Department of Transportation (DOT). (2002). "Wisconsin vehicle classification data." *Report*, Division of Transportation Investment Management, Bureau of Highway Programs, Madison, Wis.